Data Merging for Multi-Setup Operational Modal Analysis with Data-Driven SSI

M. Döhler[1], P. Andersen[2], and L. Mevel[1]

[1] *INRIA, Centre Rennes - Bretagne Atlantique, Campus de Beaulieu, F-35042 Rennes, France*

[2] *Structural Vibration Solutions A/S, NOVI Science Park, Niels Jerners Vej 10, DK-9220 Aalborg East, Denmark*

Abstract

In Operational Modal Analysis (OMA) of large structures we often need to process sensor data from multiple non-simultaneously recorded measurement setups. These setups share some sensors in common, the so-called reference sensors that are fixed for all the measurements, while the other sensors are moved from one setup to the next. To obtain the modal parameters of the investigated structure it is necessary to process the data of all the measurement setups and normalize it as the unmeasured background excitation of each setup might be different. In this paper we present system identification results using a merging technique for data-driven Stochastic Subspace Identification (SSI), where the data is merged and normalized prior to the identification step. Like this, the different measurement setups can be processed in one step and do not have to be analyzed separately. We apply this new merging technique to measurement data of the Heritage Court Tower in Vancouver, Canada.

1 Introduction

Subspace-based linear system identification methods have been proven efficient for the identification of the eigenstructure of a linear multivariable system in many applications. Our main motivation in this paper is output-only structural identification in vibration mechanics. This problem consists in identifying the modal parameters (natural frequencies, damping ratios and mode shapes) of a structure subject to ambient unmeasured vibrations, by using accelerometer measurements or strain gauges. This is output-only system identification, as the excitation input is unknown and not measured. Examples are, amongst others, offshore structures subject to swell, bridges subject to wind and traffic, etc.

We wish to analyze how the data-driven Stochastic Subspace Identification (SSI) with the Unweighted Principal Component algorithm [7] can be adapted when several successive data sets are recorded, with sensors at different locations in the structure. For doing this, some of the sensors, called the *reference sensors,* are kept fixed, while the others are moved. Like this, we mimic a situation in which lots of sensors are available, while in fact only a few are at hand. However, there is one unpleasant feature of structural identification of structures subject to ambient excitation, namely that excitation is typically turbulent in nature and nonstationary. For example, fluid/structure interaction in offshore structures results in shock effects causing nonstationary excitation, and the same holds for wind and traffic on bridges. Like this, the excitation factor can change from setup to setup.

The relevance of merging successive records, and its implementation in the case of nonstationary excitation, are the subject of this paper. We describe a new merging algorithm for data-driven SSI and test it on vibration data of the Heritage Court Tower in Vancouver, Canada.

2 Reference-based Data-driven Stochastic Subspace Identification (SSI)

2.1 Single setup

We consider a linear multi-variable output-only system described by a discrete-time state space model

$$\left\{ \begin{array}{rcl} X_{k+1} & = & F\ X_k + V_{k+1} \\ Y_k^{(\text{ref})} & = & H^{(\text{ref})}\ X_k \\ Y_k^{(\text{mov})} & = & H^{(\text{mov})}\ X_k \end{array} \right. \tag{1}$$

with

- X_k the state vector at time instant k,
- $Y_k^{(\text{ref})}$ the observed output vector of the reference sensors,
- $Y_k^{(\text{mov})}$ the observed output vector of all the sensors minus the reference sensors (the remaining sensors),
- $H^{(\text{ref})}$ the observation matrix with respect to the reference sensors,
- $H^{(\text{mov})}$ the observation matrix with respect to the remaining sensors,
- F the state transition matrix,
- V_k the unmeasured stationary Gaussian white noise.

Let furthermore

- $Y_k = \begin{pmatrix} Y_k^{(\text{ref})} \\ Y_k^{(\text{mov})} \end{pmatrix}$ all the observed output at time instant k,
- $H = \begin{pmatrix} H^{(\text{ref})} \\ H^{(\text{mov})} \end{pmatrix}$ the full observation matrix,
- N the number of measurements ($k = 1, \ldots, N$),
- r the total number of sensors and $r^{(\text{ref})}$ the number of reference sensors.

The classical reference-based data-driven subspace identification of the eigenstructure (λ, ϕ_λ) of the system (1) consists of the following steps for the Unweighted Principal Component algorithm [7]: We choose p and q as variables with $p + 1 \geq q$ that indicate the quality of the estimations (a bigger p leads to better estimates) and the maximal system order ($\leq qr^{(\text{ref})}$). Normally, we choose $p = q - 1$, but in the case of measurement noise $p = q - 1 + l$ should be chosen, where l is the order of the noise.

We build the data matrices

$$\mathcal{Y}_{p+1}^{+} \stackrel{\text{def}}{=} \begin{pmatrix} Y_{q+1} & Y_{q+2} & \vdots & Y_{N-p} \\ Y_{q+2} & Y_{q+3} & \vdots & Y_{N-p+1} \\ \vdots & \vdots & \vdots & \vdots \\ Y_{q+p+1} & Y_{q+p+2} & \vdots & Y_N \end{pmatrix}, \quad \text{and} \quad \mathcal{Y}_q^{-} \stackrel{\text{def}}{=} \begin{pmatrix} Y_q^{(\text{ref})} & Y_{q+1}^{(\text{ref})} & \vdots & Y_{N-p-1}^{(\text{ref})} \\ Y_{q-1}^{(\text{ref})} & Y_q^{(\text{ref})} & \vdots & Y_{N-p-2}^{(\text{ref})} \\ \vdots & \vdots & \vdots & \vdots \\ Y_1^{(\text{ref})} & Y_2^{(\text{ref})} & \vdots & Y_{N-p-q}^{(\text{ref})} \end{pmatrix} \tag{2}$$

and the weighted Hankel matrix[1]

$$\mathcal{H}_{p+1,q} = \mathcal{Y}_{p+1}^{+} \mathcal{Y}_q^{-T} \left(\mathcal{Y}_q^{-} \mathcal{Y}_q^{-T} \right)^{-1} \mathcal{Y}_q^{-}. \tag{3}$$

With the factorization $\mathcal{H}_{p+1,q} = \mathcal{O}_{p+1} \mathcal{X}_q$ into matrix of observability and Kalman filter state sequence with

$$\mathcal{O}_{p+1} \stackrel{\text{def}}{=} \begin{pmatrix} H \\ HF \\ HF^2 \\ \vdots \\ HF^p \end{pmatrix} \tag{4}$$

we can retrieve the matrices H as the first block row of $\mathcal{O}_{p+1}$ and F from the least squares solution of

$$\begin{pmatrix} H \\ HF \\ \vdots \\ HF^{p-1} \end{pmatrix} F = \begin{pmatrix} HF \\ HF^2 \\ \vdots \\ HF^p \end{pmatrix}.$$

[1] As $\mathcal{H}_{p+1,q}$ is usually a very big matrix and difficult to handle, we continue the calculation in practice with the R part from an RQ-decomposition of the data matrices, see [7] for details. This will lead to the same results as only the left part of the decomposition of $\mathcal{H}_{p+1,q}$ is needed.

Finally we obtain the eigenstructure (λ, ϕ_λ) of the system (1) from

$$\det(F - \lambda\, I) = 0, \quad F\, \varphi_\lambda = \lambda\, \varphi_\lambda, \quad \phi_\lambda = H\varphi_\lambda.$$

In the following we will skip the subscripts of the matrices $\mathcal{H}_{p+1,q}$, $\mathcal{Y}^+_{p+1}$, $\mathcal{Y}^-_q$ and $\mathcal{O}_{p+1}$.

2.2 Multiple setups

Instead of a single record for the output (Y_k) of the system (1), N_s records

$$\underbrace{\begin{pmatrix} Y_k^{(1,\text{ref})} \\ Y_k^{(1,\text{mov})} \end{pmatrix}}_{\text{Record } 1} \quad \underbrace{\begin{pmatrix} Y_k^{(2,\text{ref})} \\ Y_k^{(2,\text{mov})} \end{pmatrix}}_{\text{Record } 2} \quad \cdots \quad \underbrace{\begin{pmatrix} Y_k^{(N_s,\text{ref})} \\ Y_k^{(N_s,\text{mov})} \end{pmatrix}}_{\text{Record } N_s} \tag{5}$$

are now available collected successively. Each record j contains data $Y_k^{(j,\text{ref})}$ from a fixed *reference* sensor pool, and data $Y_k^{(j,\text{mov})}$ from a *moving* sensor pool. To each record $j = 1, \ldots, N_s$ corresponds a state-space realization in the form

$$\left\{ \begin{array}{lcll} X_{k+1}^{(j)} & = & F\, X_k^{(j)} + V_{k+1}^{(j)} & \\ Y_k^{(j,\text{ref})} & = & H^{(\text{ref})}\, X_k^{(j)} & (\text{reference pool}) \\ Y_k^{(j,\text{mov})} & = & H^{(j,\text{mov})}\, X_k^{(j)} & (\text{sensor pool n}^o j) \end{array} \right. \tag{6}$$

with a single state transition matrix F. Note that the unmeasured excitation $V^{(j)}$ can be different for each setup j as the environmental conditions can slightly change between the measurements. However, during each setup j the noise $V^{(j)}$ is assumed to be stationary. Note also that the observation matrix $H^{(\text{ref})}$ is independent of the specific measurement setup if the reference sensors are the same throughout all measurements $j = 1, \ldots, N_s$.

For each setup j we obtain a "local" weighted Hankel matrix

$$\mathcal{H}^{(j)} = \mathcal{Y}^+_{(j)} \mathcal{Y}^{-\,T}_{(j)} \left(\mathcal{Y}^-_{(j)} \mathcal{Y}^{-\,T}_{(j)} \right)^{-1} \mathcal{Y}^-_{(j)} \tag{7}$$

according to equations (2)-(3), where $\mathcal{Y}^+_{(j)}$ is filled with data from all the sensors and $\mathcal{Y}^-_{(j)}$ with data from the reference sensors of this setup (see Equation (2)). The question is now how to adapt the subspace identification from Section 2.1 to

- merge the data from the multiple setups $j = 1, \ldots, N_s$ to obtain global modal parameters (natural frequencies, damping ratios, mode shapes), and to
- normalize or re-scale the data from the multiple setups as the background excitation may differ from setup to setup.

In the following section we present two approaches for this problem: the common practice approach PoSER that processes all the setups separately and merges them at the end, and the new approach PreGER, that processes all the setups together.

3 Merging strategies

3.1 PoSER approach with UPC

When having multiple measurement setups that share some reference sensors, it is common practice to perform the subspace identification algorithm of Section 2.1 on each setup separately in order to obtain the (local) modal parameters. To obtain the natural frequencies and damping ratios of the whole structure, the appropriate values of all setups are averaged. In order to merge the obtained (partial) mode shapes, we have to re-scale them as they were calculated on excitation factors that were possibly different from setup to setup. This is done in a least-square sense on the reference sensor part of each partial mode shape. This approach is also called *PoSER* (Post Separate Estimation Re-scaling), see also e.g. [6].

Especially when the number of setups is large, this approach can be tiresome as many stabilization diagrams have to be analyzed. Some modes may be less excited in some of the setups, and it might be difficult to distinguish closely spaced modes in the diagrams.

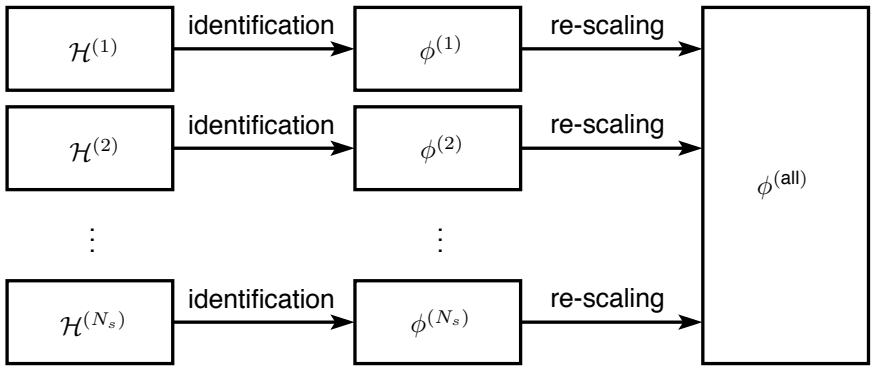

Figure 1: Merging partial mode shape estimates $\phi^{(j)}$, $j = 1, ..., N_s$ into a global mode shape estimate $\phi^{(\text{all})}$ in the PoSER approach.

3.2 PreGER approach with UPC

Another merging approach that was described for covariance-driven SSI in [4, 5, 2] makes use of a factorization of the Hankel matrix of each setup and normalizes them with a common right factor to introduce the same excitation factor to all the setups. We adapt this idea to the data-driven SSI with the UPC algorithm. We also call this method *PreGER* (Pre Global Estimation Re-scaling).

For each setup $j = 1, \ldots, N_s$ we build the weighted Hankel matrix (7) that has the factorization property $\mathcal{H}^{(j)} = \mathcal{O}^{(j)}\mathcal{X}^{(j)}$. In order to merge the data we first take the different excitation factors of each setup into account, which are present in the Kalman filter state sequence $\mathcal{X}^{(j)}$ since the matrix of observability is only dependent of the observation matrix $H^{(j)}$ and state matrix F that are not affected. In the first step, all the Hankel matrices $\mathcal{H}^{(j)}$ are re-scaled with a common Kalman filter state sequence $\mathcal{X}^{(j^*)}$ of one fixed setup j^*, then the resulting matrices are merged and a global modal parameter estimation is finally done on the merged matrix.

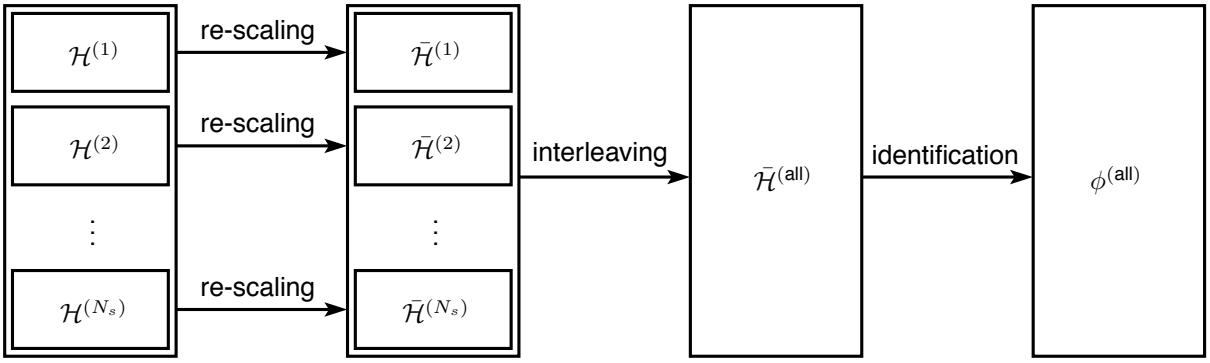

Figure 2: Merging Hankel matrices of each setup to obtain a global Hankel matrix and global mode shape estimate $\phi^{(\text{all})}$ in the PreGER approach.

In detail, we separate the weighted Hankel matrices $\mathcal{H}^{(j)}$ into matrices $\mathcal{H}^{(j,\text{ref})}$ and $\mathcal{H}^{(j,\text{mov})}$ by taking the appropriate rows of $\mathcal{H}^{(j)}$ that correspond to the reference resp. moving sensor data from $\mathcal{Y}^{+}_{(j,\text{ref})}$ resp. $\mathcal{Y}^{+}_{(j,\text{mov})}$, see also Equation (7). As the weighted Hankel matrices fulfill the factorization property $\mathcal{H}^{(j)} = \mathcal{O}^{(j)}\mathcal{X}^{(j)}$ we now have

$$\mathcal{H}^{(j,\text{ref})} = \mathcal{O}^{(\text{ref})}\mathcal{X}^{(j)}, \quad \mathcal{H}^{(j,\text{mov})} = \mathcal{O}^{(j,\text{mov})}\mathcal{X}^{(j)},$$

with the matrices of observability

$$\mathcal{O}^{(j)} = \begin{pmatrix} H^{(j)} \\ H^{(j)}F \\ H^{(j)}F^2 \\ \vdots \\ H^{(j)}F^p \end{pmatrix}, \quad \mathcal{O}^{(\text{ref})} = \begin{pmatrix} H^{(\text{ref})} \\ H^{(\text{ref})}F \\ H^{(\text{ref})}F^2 \\ \vdots \\ H^{(\text{ref})}F^p \end{pmatrix}, \quad \mathcal{O}^{(j,\text{mov})} = \begin{pmatrix} H^{(j,\text{mov})} \\ H^{(j,\text{mov})}F \\ H^{(j,\text{mov})}F^2 \\ \vdots \\ H^{(j,\text{mov})}F^p \end{pmatrix}.$$

Note also, that $\mathcal{O}^{(j)}$ consists of the rows of $\mathcal{O}^{(j,\text{ref})}$ and $\mathcal{O}^{(j,\text{mov})}$. For the normalization we need the matrices $\mathcal{X}^{(j)}$ in the same state basis. We juxtapose the matrices $\mathcal{H}^{(j,\text{ref})}$, $j = 1, \ldots, N_s$ to

$$\mathcal{H}^{(\text{all,ref})} = \begin{pmatrix} \mathcal{H}^{(1,\text{ref})} & \mathcal{H}^{(2,\text{ref})} & \ldots & \mathcal{H}^{(N_s,\text{ref})} \end{pmatrix}$$

and decompose this matrix to

$$\mathcal{H}^{(\text{all,ref})} = \mathcal{O}^{(\text{ref})} \begin{pmatrix} \mathcal{X}^{(1)} & \mathcal{X}^{(2)} & \ldots & \mathcal{X}^{(N_s)} \end{pmatrix},$$

from where we obtain the matrices $\mathcal{X}^{(j)}$. We choose one setup $j^* \in \{1, \ldots, N_s\}$ and re-scale the matrices $\mathcal{H}^{(j,\text{mov})}$ to

$$\bar{\mathcal{H}}^{(j,\text{mov})} = \mathcal{H}^{(j,\text{mov})} \; {\mathcal{X}^{(j)}}^T (\mathcal{X}^{(j)} \; {\mathcal{X}^{(j)}}^T)^{-1} \; \mathcal{X}^{(j^*)},$$

so that $\bar{\mathcal{H}}^{(j,\text{mov})} = \mathcal{O}^{(j,\text{mov})} \mathcal{X}^{(j^*)}$ holds. In the last step we interleave the block rows of the matrices $\bar{\mathcal{H}}^{(j,\text{mov})}$, $j = 1, \ldots, N_s$, and the matrix $\mathcal{H}^{(j^*,\text{ref})}$, to obtain the merged matrix $\bar{\mathcal{H}}^{(\text{all})}$ with the factorization property

$$\bar{\mathcal{H}}^{(\text{all})} = \mathcal{O}^{(\text{all})} \; \mathcal{X}^{(j^*)} \quad \text{with} \quad \mathcal{O}^{(\text{all})} = \begin{pmatrix} H^{(\text{all})} \\ H^{(\text{all})}F \\ H^{(\text{all})}F^2 \\ \vdots \\ H^{(\text{all})}F^p \end{pmatrix} \quad \text{and} \quad H^{(\text{all})} = \begin{pmatrix} H^{(\text{ref})} \\ H^{(1,\text{mov})} \\ H^{(2,\text{mov})} \\ \vdots \\ H^{(N_s,\text{mov})} \end{pmatrix}$$

and perform the subspace system identification on it to obtain the global modal parameters.

4 Modal analysis of the Heritage Court Tower

4.1 Description of the Heritage Court Tower and vibration measurements

The building considered in this study is the Heritage Court Tower (HCT) in downtown Vancouver, British Columbia in Canada. It is a relatively regular 15-story reinforced concrete shear core building. In plan, the building is essentially rectangular in shape with only small projections and setbacks. Typical floor dimensions of the upper floors are about 25 m by 31 m, while the dimensions of the lower three levels are about 36 m by 30 m. The footprint of the building below ground level is about 42 m by 36 m. Typical story heights are 2.70 m, while the first story height is 4.70 m. The elevator and stairs are concentrated at the center core of the building and form the main lateral resisting elements against potential wind and seismic lateral and torsional forces. The tower structure sits on top of four levels of reinforced concrete underground parking. The parking structure extends approximately 14 meters beyond the tower in the south direction forming an L-shaped podium. The parking structure and first floors of the tower are basically flush on the remaining three sides. The building tower is stocky in elevation having a height to width aspect ratio of approximately 1.7 in the east-west direction and 1.3 in the north-south direction. Because the building sits to the north side of the underground parking structure, coupling of the torsional and lateral modes of vibration was expected primarily in the EW direction.

As reported in [8], a series of ambient vibration tests was conducted on April 28, 1998 by researchers from the University of British Columbia [3]. It was of practical interest to test this building because of its shear core, which concentrates most of lateral and torsional resisting elements at the center core of the building. Additional structural walls are located close to the perimeter of the building but are arranged in such a way that they offer no additional torsional restraint. Shear core buildings may exhibit increased torsional response when subjected to strong earthquake motion depending on the uncoupled lateral to torsional frequency ratio and of the amount of static eccentricity in the building plan [1]. The dynamic characteristics of interest for this study were the first few lateral and torsional natural frequencies and the corresponding mode shapes. The degree of torsional coupling between the modes was also investigated.

The vibration measurements were conducted using an eight-channel system (with force-balanced accelerometers) and were recorded in four different measurement setups. The accelerometers were typically located in the northwest and northeast corners of the building on every other floor starting from the roof down to the ground floor. Details of the field testing of this structure are given in [3].

Figure 3: HCT Building and setup close up

4.2 Modal analysis with the PoSER and PreGER approaches

The modal analysis for both the PoSER and PreGER approach was tuned with the same parameters. The maximal considered model order was 80 and the number of samples was 6560 and hence relatively low, amounting to 328s at a sampling rate of 20Hz. The parameters for the modal extraction from the stabilization diagrams are shown in Figure 4.

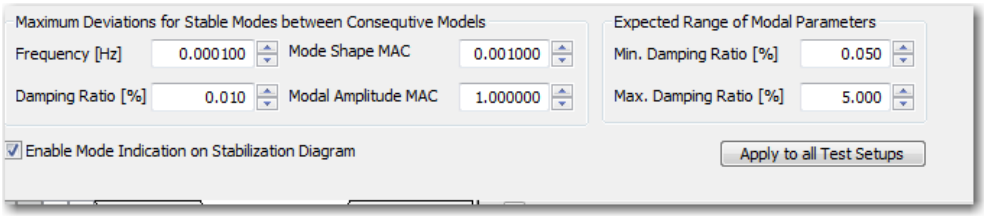

Figure 4: Tuning of the SSI approach

In the PoSER approach all the four setups are processed separately, as described in Section 3.1. In the PreGER approach all the four setups are processed at once, as described in Section 3.2. The resulting stabilization diagrams are shown in Figures 5 and 6.

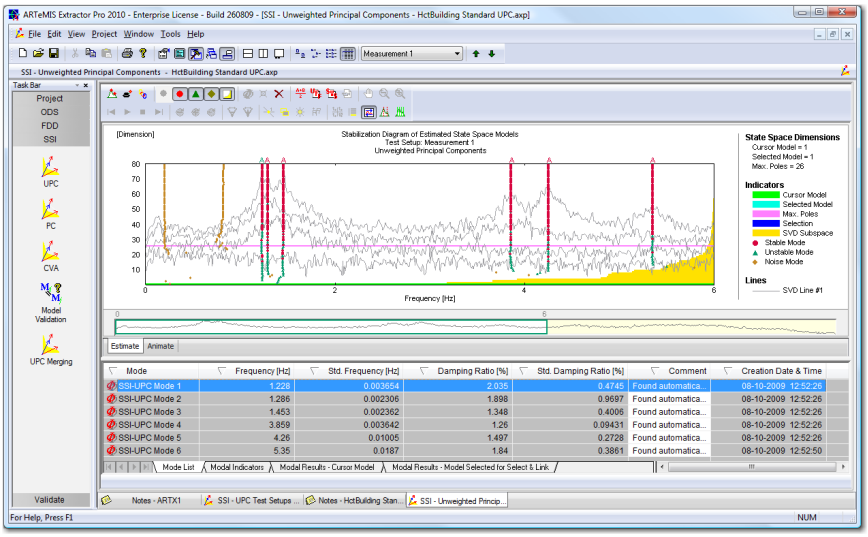

Figure 5: PoSER stabilization diagram.

Figure 6: PreGER stabilization diagram.

In the frequency range of interest [0 – 6 Hz], 6 modes could be identified. Their natural frequencies and damping ratios are displayed in Tables 1 and 2. A comparison to the natural frequencies obtained by [8] together with the characteristics of the corresponding mode shapes is given in Table 3.

Mode	Frequency [Hz]	Damping Ratio
1	1.228	2.035
2	1.286	1.898
3	1.453	1.348
4	3.859	1.260
5	4.260	1.497
6	5.350	1.840

Table 1: Identified modes with the PoSER approach.

Mode	Frequency [Hz]	Damping Ratio
1	1.229	2.914
2	1.295	2.466
3	1.449	1.516
4	3.855	1.491
5	4.258	2.242
6	5.369	2.928

Table 2: Identified modes with the PreGER approach.

Mode No.	EMA freq.	Mode type
1	1.23	1st NS mode
2	1.27	1st Torsional
3	1.44	1st EW mode
4	3.87	2nd Torsional (coupled)
5	4.25	2nd NS mode
6	5.35	2nd EW mode (coupled)

Table 3: EMA modes and mode shape descriptions [8].

For all modes, the damping ratios of the PreGER estimates are somewhat higher than the PoSER estimates. This might be due to the fact, that the natural frequencies in each measurement setup are slightly different. Then, the resulting frequency for each mode obtained by the PreGER approach is associated to a higher damping ratio, consequence from the merging of overlapping frequencies.

The mode shapes obtained by the PoSER and PreGER approaches are shown in Figure 8 and a MAC comparison between them is shown in Figure 7. The MAC values are very close to 1, indicating very similar mode shapes.

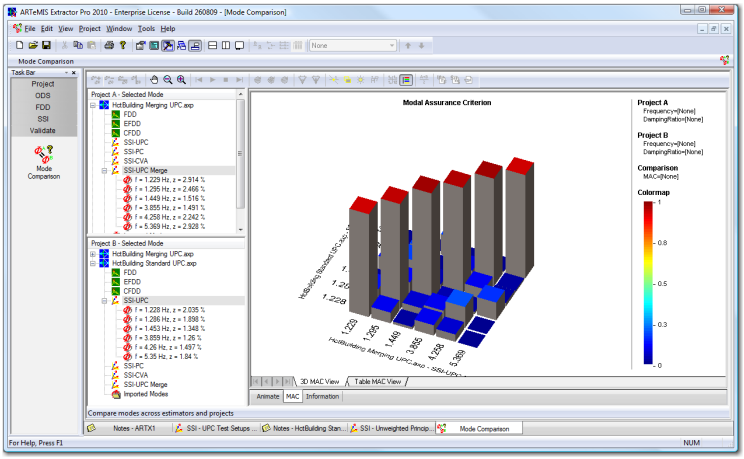

Figure 7: MAC between mode shapes estimated by PoSER and PreGER approaches.

5 Summary of results

This paper focuses on obtaining the full mode shapes from a structure, under the assumption that sensor measurements were collected in different sessions. Two approaches were considered, both based on the data-driven SSI framework. The first approach, PoSER, merges the mode shapes obtained on the different setups after the SSI of each setup, while the second approach, PreGER, merges the correlation of the data before performing the SSI on the full set of data. All modes were recovered, damping estimates were consistent, albeit a bit higher for the PreGER approach, which is expected. As for the mode shapes, good MAC coherency was obtained between the two methods. The PreGER approach shows good prospect because it does not need any post processing of the estimation results in order to get the full mode shapes of the structure and no threshold based matching of modes between setups is needed.

mode 1 - 1.229 Hz - 2.97 %

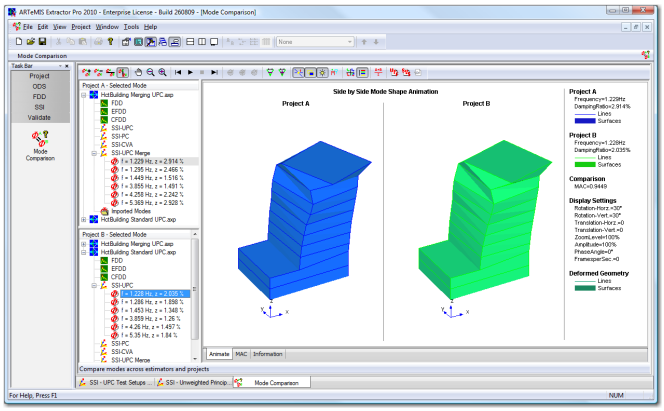

mode 2 - 1.295 Hz - 2.48 %

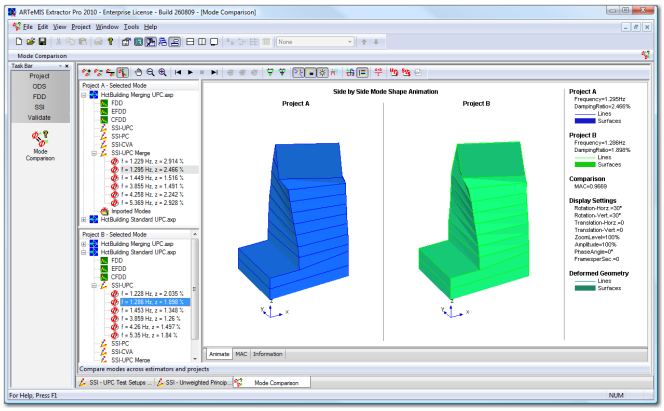

mode 3 - 1.448 Hz - 2.57 %

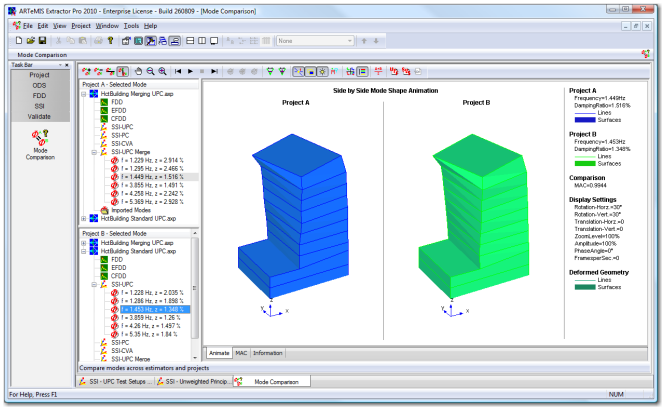

mode 4 - 3.855 Hz - 1.50 %

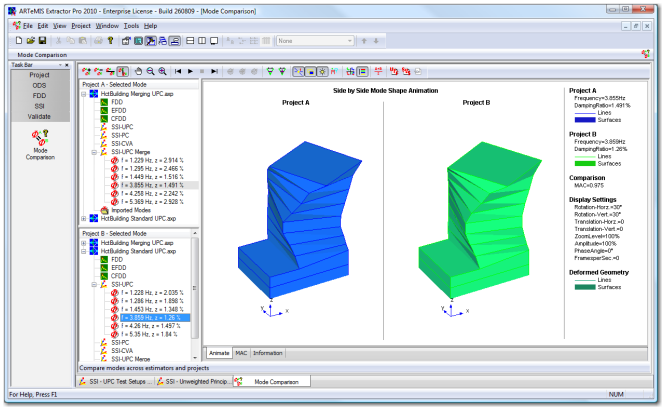

mode 5 - 4.258 Hz - 2.26 %

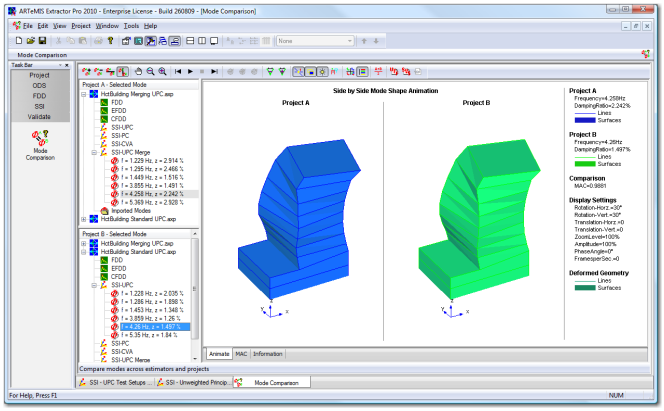

mode 6 - 5.369 Hz - 2.95 %

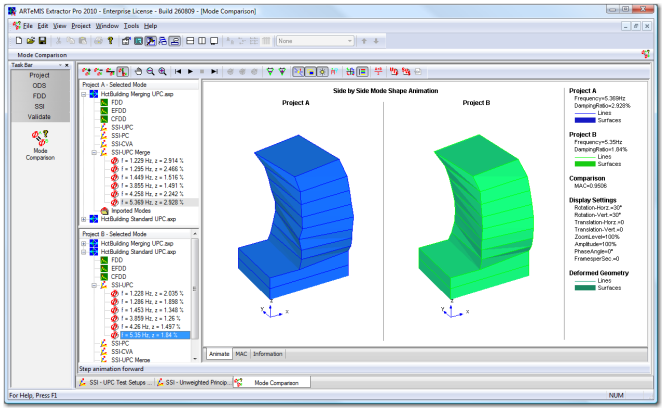

Figure 8: First 6 mode shapes obtained with the PoSER and the PreGER approach.

References

[1] J. de la Llera and A. Chopra. *Accidental and natural torsion in earthquake response and design of buildings*. Earthquake Engineering Research Center, University of California, 1994.

[2] M. Döhler, E. Reynders, F. Magalhães, L. Mevel, G. D. Roeck, and A. Cunha. Pre- and post-identification merging for multi-setup OMA with covariance-driven SSI. In *Proceedings of IMAC 28, the International Modal Analysis Conference*, Jacksonville, FL, 2010.

[3] C. Dyck and C. Ventura. Ambient Vibration Measurements of Heritage Court Tower. *EQ LAB, University of British Columbia, Earthquake Engineering Research*, 1998.

[4] L. Mevel, M. Basseville, A. Benveniste, and M. Goursat. Merging sensor data from multiple measurement setups for nonstationary subspace-based modal analysis. *Journal of Sound and Vibration*, 249(4):719–741, 2002.

[5] L. Mevel, A. Benveniste, M. Basseville, and M. Goursat. Blind subspace-based eigenstructure identification under nonstationary excitation using moving sensors. *IEEE Transactions on Signal Processing*, SP-50(1):41–48, 2002.

[6] E. Reynders, F. Magalhães, G. D. Roeck, and A. Cunha. Merging strategies for multi-setup operational modal analysis: application to the Luiz I steel arch bridge. In *Proceedings of IMAC 27, the International Modal Analysis Conference*, Orlando, FL, 2009.

[7] P. Van Overschee and B. De Moor. *Subspace Identification for Linear Systems: Theory, Implementation, Applications*. Kluwer, 1996.

[8] C. Ventura, R. Brincker, E. Dascotte, and P. Andersen. FEM updating of the heritage court building structure. In *Proceedings of IMAC 19, the International Modal Analysis Conference*, volume 1, pages 324–330, 2001.